

Measurement of a topological edge invariant in a microwave network

Wenchao Hu,¹ Jason C. Pillay,² Kan Wu,³ Michael Pasek,² and Y. D. Chong^{1,2,*}

¹*Centre for Disruptive Photonic Technologies, Nanyang Technological University, Singapore 637371, Singapore*

²*Division of Physics and Applied Physics, School of Physical and Mathematical Sciences, Nanyang Technological University, Singapore 637371, Singapore*

³*State Key Laboratory of Advanced Optical Communication Systems and Networks, Department of Electronic Engineering, Shanghai Jiao Tong University, Shanghai 200240, China*

We report on the measurement of topological invariants in an electromagnetic topological insulator analog formed by a microwave network, consisting of the winding numbers of scattering matrix eigenvalues. The experiment can be regarded as a variant of a topological pump, with non-zero winding implying the existence of topological edge states. In microwave networks, unlike most other systems exhibiting topological insulator physics, the winding can be directly observed. The effects of loss on the experimental results, and on the topological edge states, is discussed.

PACS numbers: 42.60.Da, 42.70.Qs, 73.43.-f

I. INTRODUCTION

Topological insulators are phases of matter that are “topologically distinct” from conventional insulators, meaning that their electronic bandstructures cannot be deformed into conventional bandstructures without closing bandgaps. This allows different phases to exist without symmetry breaking, in contravention of the long-established Landau theory of phase transitions. Topologically nontrivial bandstructures were originally discovered in the condensed matter context, first in the quantum Hall (QH) effect [1] and then in 2D and 3D materials with strong spin-orbit coupling [2]. Recently, the concept has even been extended to photonics, with coherent classical electromagnetic fields taking the place of single-electron wavefunctions. Such “topological photonics” devices have been experimentally realized with microwave-scale gyromagnetic photonic crystals [3–6], and, at optical and infrared frequencies, with coupled waveguide lattices [7] and coupled resonator lattices [8, 9]. There have also been theoretical proposals based on modulated photonic crystal resonances [10], circuit QED systems [11, 12], metamaterial photonic crystals [13], etc. Typically, the key experimental signature of a topologically nontrivial photonic bandstructure is taken to be the presence of robust transmission along the edge of a sample, independent of sample geometry and defects. This relies on the theoretical principle of “bulk-edge correspondence”, which relates the number of topological edge states within each bandgap to topological invariants that characterize the topology of the bulk bands.

In condensed matter systems, another strong indicator of nontrivial band topology is the rigid quantization of certain macroscopic transport properties. Most famously, in the integer QH effect [14], the Hall resistance is quantized to inverse integer multiples of the von Klitzing constant. An influential explanation for this was

supplied by Thouless and co-workers [15], who showed that in linear response theory the QH conductance is linked to the Chern number invariants of the bulk bands, which take integer values. In photonics, linear response-based measurements are unphysical, because there is no fermionic ground state. There is, however, another link between the QH effect and topology which does *not* rely on linear response theory, and can usefully be extended to electromagnetism. This is Laughlin’s adiabatic pumping thought experiment, in which single-electron wavefunctions are adiabatically transported across a sample by a gauge transformation, and the robustness of the QH effect is explained in terms of the quantization of the transported current due to gauge invariance [16].

In this paper, we present experimental measurements of topological edge invariants in a microwave network, in the form of winding numbers of scattering matrix (S matrix) eigenvalues measured at the edges of the network. This experiment is a variant of the adiabatic pump [16], reformulated in terms of scattering processes [17–19], which is a particularly natural approach for dealing with electromagnetic systems. In the context of periodic networks, two of the authors have previously shown that such an experiment acts as a probe of the network’s “quasi-energy” bandstructure and its edge states [20]. It is remarkable that, even though adiabatic pumping is typically regarded as a “thought experiment”, it can actually be implemented in electromagnetic systems. Recently, an adiabatic pumping scheme has been demonstrated in quasicrystalline optical waveguide arrays [21, 22], and a related scheme based on a ring of coupled optical resonators has been proposed by Hafezi [23]. Compared to these previous works, our microwave network setup is noteworthy in that the measurements are not limited to intensities, but include full phase information, since the complex S matrix can be determined with a microwave network analyzer; this allows the complex winding process to be directly observed. Furthermore, our setup provides a convenient platform for studying the topological properties of quasi-energy bandstructures, a topic of recent theoretical interest [24–30].

* yidong@ntu.edu.sg

The remainder of this paper is organized as follows: Section II reviews the theory of network bandstructures and their topological properties; Section III describes the experimental setup and results; finally, Section IV discusses the implications of the experiment, including how we can understand the effects of losses on the topological edge invariant and the network bandstructure.

II. BANDSTRUCTURES AND TOPOLOGICAL PUMPS IN NETWORKS

A network model describes a lattice in terms of wave amplitudes undergoing unitary scattering, instead of eigenstates of a Hamiltonian. Such models were originally introduced into the QH literature as a method for studying disorder in QH systems [31] (and, subsequently, in other types of topological insulators [32, 33]), by abstracting away many irrelevant details of the disordered Hamiltonians. As it turns out, they also provide a natural and accurate way to describe certain electromagnetic systems, in lieu of approximate Hamiltonian models [20, 34]. They are also theoretically interesting because their mathematical descriptions map onto the recently-proposed class of “Floquet” topological insulators, in which topological behavior is induced by time-periodic driving fields [24–30].

In this work, we are concerned with periodic, disorder-free directed networks, such as that shown schematically in Fig. 1(a). This network consists of a two-dimensional (2D) square lattice, with four directed links per unit cell. A “solution” to the network is a set of complex wave amplitudes, defined along the links, such that (i) traversing each link incurs a fixed phase delay ϕ and (ii) the amplitudes entering and leaving each node are related by a fixed 2×2 unitary coupling matrix. In the infinite network, one looks for solutions obeying Bloch’s theorem, and for each quasimomentum $[k_x, k_y]$ there exist solutions for discrete values of the phase delay ϕ (with all other aspects of the network, including the coupling matrices, fixed). We can regard ϕ as a “quasi-energy” which acts like the energy in a Hamiltonian system, except that it is an angle variable [20, 34].

The network model concept is closely related to a photonic QH analog recently proposed and realized by Hafezi *et al.*, consisting of a lattice of coupled optical resonators [8, 9]. Those authors showed that in the tight-binding (Hamiltonian) limit, a synthetic magnetic vector potential can be engineered into the hoppings between adjacent optical resonators, by coupling the resonators using auxilliary waveguides that have asymmetrical arm lengths. When the arm lengths vary incommensurately with the lattice period, the tight-binding Hamiltonian model for the resonator modes maps to that of an electron in a lattice with an applied magnetic field. This implies the existence of robust electromagnetic edge states analogous to QH edge states, which have dually been observed [9]. Surprisingly, however, even if the auxilliary

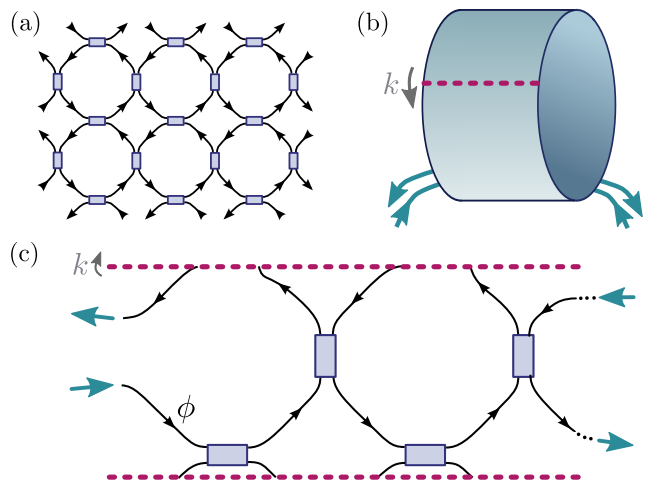


FIG. 1. (a) Schematic of a periodic 2D directed network. Wave amplitudes undergo phase delay ϕ along each directed link (black arrows), and couple through a 2×2 unitary matrix at each node (blue boxes). (b) In an adiabatic pumping setup, a 2D system is rolled into a cylinder; twisted boundary conditions with tunable twist angle k are applied, and a transport measurement is performed in the axial direction (cyan arrows). (c) Adiabatic pumping setup for a network model, with a cylinder comprising one unit cell in the azimuthal direction and two cells in the axial direction.

waveguides are chosen to be symmetrical and commensurate (corresponding to zero “magnetic flux”), the system can still exhibit robust one-way edge states, as has been demonstrated via finite-difference time-domain simulations of Maxwell’s equations [35], though not yet experimentally to our knowledge. The explanation for this can be obtained by moving beyond the tight-binding description, and modeling the system as a network [20, 34, 35]. The network’s quasi-energy bandstructure turns out to be topologically nontrivial when the inter-resonator coupling strength (described by a parameter in the coupling matrices) exceeds a critical value, corresponding to the Chalker-Coddington critical point for classical percolation through the network [31].

In the present experiment, a network is implemented with coaxial cables (links) attached to directional couplers (nodes). Each node is implemented as a single 2×2 coupler, without the auxilliary waveguides used in the resonator lattice of Hafezi *et al.* In that system, the auxilliary waveguides were required to conserve the chirality of the resonator modes in adjacent unit cells, since the resonators were on-chip structures; in the microwave network, the same thing can be achieved by merely attaching the couplers in the appropriate order.

An adiabatic pumping experiment consists of rolling a 2D lattice into a cylinder, implementing a twist in the azimuthal boundary conditions, and performing a transport measurement in the axial direction (i.e., at the edges of the cylinder). This is shown schematically in Fig. 1(b). In the original Laughlin formulation, the twist comes from the Aharonov-Bohm phase induced by threading

magnetic flux through the cylinder, and the measured quantity is the number of electrons transported in the axial direction; by gauge invariance, a 2π twist (from threading one magnetic flux quantum) corresponds to an integer number of transported electrons, and from this the quantization of the Hall conductance can ultimately be derived [16]. In our microwave network, a tunable twist k is achieved by connecting the cables at each end of the “azimuthal axis” to phase shifters. We measure the complex scattering parameters along the axis (i.e., the reflection and transmission coefficients for microwave signals injected into the edges of the cylinder), thus obtaining the S matrix, which is 2×2 in the present network geometry. In the ideal situation where the network is completely lossless, S is unitary, and its eigenvalues σ_{\pm} lie on the unit circle in the complex plane. If the quasi-energy ϕ lies in a bandgap, and the cylinder is sufficiently long, then the transmission goes to zero, and σ_{\pm} reduce to the reflection coefficients from each of the two edges. Then the winding numbers of σ_{\pm} , as the twist angle k is tuned through 2π , are the desired integer invariants, which can be shown to correspond to the number of topologically-protected one-way edge states residing on that edge [17–20].

A similar idea for observing adiabatic pumping in a photonic system has recently been advanced by Hafezi [23]. In this theoretical proposal, coupled ring resonators are placed in an annular arrangement, and as the phase shift along one column in the annulus is tuned through 2π , a set of transmission peaks is transported through one period in the transmission spectrum (measured along the edge of the annulus). This proposal is closely analogous to the original Laughlin conception of pumping electronic states [16]. An adiabatic pump has also been realized experimentally using a quasicrystalline optical waveguide array, which can be mapped onto a 2D QH system [21, 22]. The present experiment, by contrast, is based on the above-mentioned scattering formulation; our goal will be to observe the emergence of an integer invariant in the form of the winding number of a scattering parameter.

III. EXPERIMENTAL SETUP AND RESULTS

Our experimental setup is shown in Fig. 2. The network is divided into identical subunits, each consisting of 4 cables, 2 phase shifters, and 2 couplers. By comparison with Fig. 1(c), each subunit is equivalent to a “cylinder” in the adiabatic pumping setup that is one cell wide and one cell long. Connecting the subunits in series forms a longer cylinder; Fig. 2 shows a “two-cell” configuration. The cables are standard low-loss coaxial RF cables of ~ 15 cm length, and the couplers are four-port single-directional couplers, with isolators built into each port and coupling ratios of approximately 90:10 (DTO-2.5/5-10, Shanghai Huaxiang Computer Ltd.). The two phase shifters in each cell (TKE-90-6SA, Shanghai Huaxiang Computer Ltd.) are independently tunable, and set to

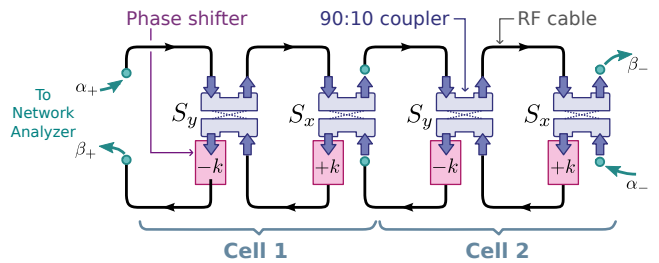


FIG. 2. Experimental setup. Each of the identical units, labelled here “Cell 1” and “Cell 2”, corresponds to one cell in the adiabatic pumping geometry of Fig. 1. A pair of phase shifters in each cell (pink boxes), with shifts of $+k$ and $-k$ respectively, implement the twisted boundary condition. The couplers (blue rods) are depicted in the “strong coupling” configuration; the “weak coupling” configuration is achieved by swapping each coupler’s outputs. The overall input and output amplitudes are α_{\pm} and β_{\pm} ; their scattering parameters are measured with a network analyzer.

produce $+k$ and $-k$ phase shifts respectively. The operating frequency is chosen to be 5 GHz, low enough to reduce losses in the various components while high enough to allow phase shifts in the full range $k \in [0, 2\pi]$. There is one input port and one output port at each end of the network, connected to a vector network analyzer (Anritsu 37396C). From this, we measure the S matrix, defined as

$$S \begin{bmatrix} \alpha_+ \\ \alpha_- \end{bmatrix} = \begin{bmatrix} \beta_+ \\ \beta_- \end{bmatrix}, \quad (1)$$

where $\{\alpha_{\pm}, \beta_{\pm}\}$ are the input and output wave amplitudes at the two edges, as labeled in Fig. 2.

Since the couplers have fixed coupling ratios, we are unable to continuously vary the network’s coupling strength parameter, on which the bandstructure topology depends. However, by swapping the order of each coupler’s output ports, we can switch between the two cases of a topologically trivial and nontrivial bandstructure. As described in Ref. 34, the coupling strength in a square lattice network can be described by a parameter $\theta \in [0, \pi/2]$ in the coupling matrices of the node couplers, where $\theta = 0$ is zero coupling and $\pi/2$ is complete coupling. The bandstructure is topologically trivial for $\theta < 0.25\pi$, and nontrivial for $\theta > 0.25\pi$, independent of all other coupling matrix parameters. Our 90:10 couplers thus allow for either $\theta \approx \tan^{-1}(3) \approx 0.40\pi$ (topologically nontrivial; this is the configuration shown in Fig. 2) or $\theta \approx \tan^{-1}(1/3) \approx 0.10\pi$ (topologically trivial). At the 5 GHz operating frequency, each cable has phase delay $\approx 0.2\pi$, which lies in a bandgap of the quasi-energy bandstructure for both the strong and weak-coupling cases. The loss in each cable is ≈ 0.4 dB.

The measured S matrix eigenvalues are shown in Fig. 3. The eigenvalues do not lie on the unit circle, due to losses in the network which make the S matrix sub-unitary. Nonetheless, the eigenvalue trajectories exhibit winding behaviors very similar to the lossless case.

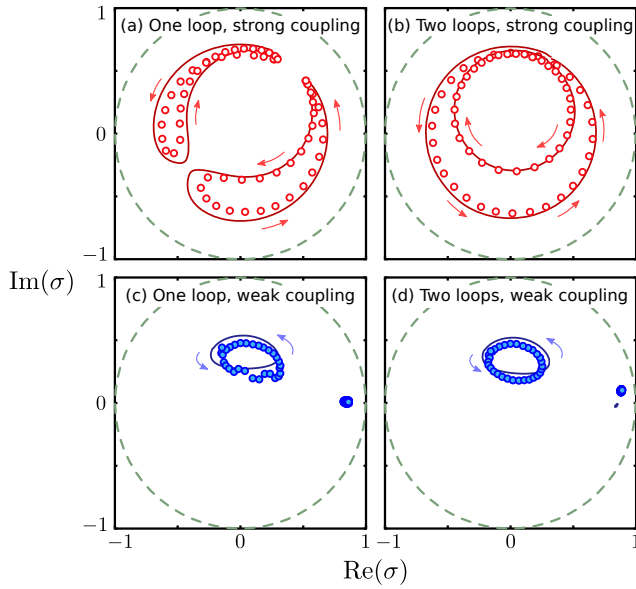


FIG. 3. Scattering matrix eigenvalues measured across one cell (left) and across two cells in series (right). Arrows indicate the direction of motion with increasing k . Circles show experimental data; solid curves show theoretical calculations using the scattering parameters measured for each network component individually (including losses). Non-zero winding numbers can be observed in the strong-coupling two-cell case. The unit circle is indicated by dashed curves.

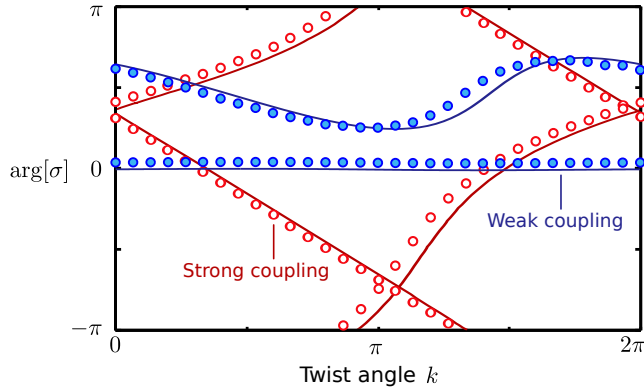


FIG. 4. Arguments of the complex S matrix eigenvalues for the two-cell network, as the phase shift k is tuned through 2π . Empty circles show the strong coupling measurement data, and filled circles show the weak coupling data; solid curves show theoretical calculations. For strong coupling, the two eigenvalues have winding numbers ± 1 , corresponding to the bulk bandstructure being topologically nontrivial.

For the one-cell system under strong coupling, the two S matrix eigenvalues, σ_{\pm} , move along distinct closed trajectories as k is increased through 2π , as shown in Fig. 3(a). Each individual trajectory does not encircle the origin (i.e. the winding number is zero), even though the network bandstructure is in the topologically nontrivial regime. This is because topological protection re-

quires the opposite edges in a finite system to be well separated, so as to have negligible overlap between the counter-propagating edge states on each edge. When the separation is increased by connecting two cells in series, the trajectories coalesce into a pair of loops with winding numbers ± 1 , as shown in Fig. 3(b). By contrast, in the weak coupling regime of Figs. 3(b) and 3(d), the eigenvalues move along separate trajectories without encircling the origin. The winding number can also be visualized by plotting $\arg[\sigma_{\pm}]$ against k , as in Fig. 4.

IV. DISCUSSION

Our experiment deviates from an ideal adiabatic pump in several respects. Firstly, as previously mentioned, in the ideal adiabatic pumping experiment the edges are separated by a large number of unit cells, so that there is a true “bulk”, whereas in our experiment there are only two unit cells. However, this does not make a significant difference to the physical interpretation, as the relevant phenomenon—the emergence of a non-zero winding number—is observed already when going from the one-cell to the two-cell case, shown in Figs. 3(a) and (b). This arises from the fact that the system is deep in either the topologically trivial or nontrivial phases, based on our choices of the coupling strength θ ; in the nontrivial case, each edge state is strongly confined to one unit cell, with negligible amplitude on the next unit cell. Indeed, calculations based on realistic parameters show no significant changes in the trajectory of the S matrix eigenvalues as the number of cells is increased beyond two.

Another difference between our experiment and the ideal adiabatic pump is the presence of loss in all the network components: the cables, phase shifters, and couplers. As a result, the eigenvalues of the S matrix are not strictly constrained to the unit circle, as seen in Fig. 3. Nonetheless, we argue that these eigenvalue trajectories can be meaningfully linked to the existence or non-existence of topological edge states, based on the close relationship between the edge scattering parameters measured in the experiment and the projected bandstructure of the network.

When the edges are well-separated, the S matrix reduces to a pair of reflection coefficients $r_{\pm} \equiv \beta_{\pm}/\alpha_{\pm}$, where $\{\alpha_{\pm}, \beta_{\pm}\}$ are the input/output wave amplitudes labeled in Fig. 2. In the experiment, r_{\pm} is determined based on two parameters ϕ and k , with all other parameters (such as the coupling matrices) fixed; varying k then gives results like those shown in Fig. 3 and Fig. 4. Alternatively, we could either (i) determine ϕ given r_{\pm} and k (by finding the eigenvalues of the scattering matrix for one period of an infinite strip [20]), or (ii) determine k given r_{\pm} and ϕ (by finding the eigenvalues of the transfer matrix for one period of the strip). Both of these procedures yield the projected bandstructure, with r_{\pm} interpreted not as reflection coefficients, but as *boundary conditions* which are applied along the edge of the strip,

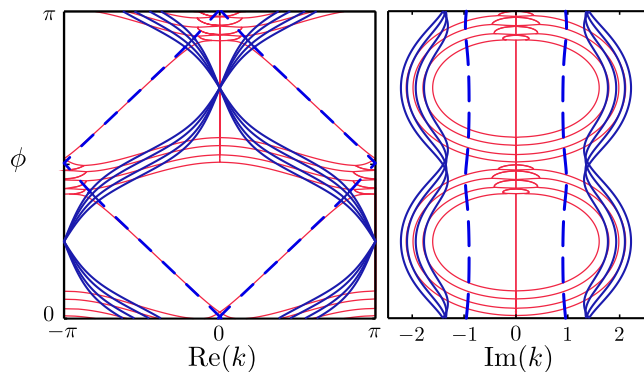


FIG. 5. Complex projected bandstructure of a hypothetical lossy network (blue lines), consisting of an infinite strip 5 unit cells wide. Each link has real tunable phase delay ϕ , each coupler has loss $e^{-\gamma}$ in each output port where $\gamma = 0.25$, and each edge of the strip obeys lossy boundary conditions $r_{\pm} = \exp(-0.2\pi)$, chosen to be roughly the same as in the experiment. The coupling strength is $\theta = 0.4\pi$, approximately equal to the “strong coupling” (topologically nontrivial) configuration in the experiment. The bandstructure for the lossless network ($\gamma = 0$ and $|r_{\pm}| = 1$) is plotted for comparison (red lines). The lossy network exhibits edge states whose dispersion relations are almost identical to the lossless network’s topological edge states, and have lower loss than all other states (blue dashes).

specifying the phase shifts on the edge links. In the absence of losses, if the scattering experiment yields a non-zero winding number for ϕ in a bulk bandgap, then it can be seen that the projected bandstructure exhibits topological edge states [20]. Now consider a lossy network. The losses can be described, without loss of generality, by making the coupling matrices sub-unitary, as well as by setting $|r_{\pm}| < 1$ (lossy boundary conditions). The above two procedures, (i) and (ii), lead to two distinct types of complex projected bandstructure; we focus on procedure (ii), which takes r_{\pm} and a real ϕ and yields complex wave-numbers k , whose imaginary parts are the attenuation constants of the propagating modes. One such complex bandstructure is shown in Fig. 5, generated using representative lossy r_{\pm} and coupling matrices (a 5-cell-wide strip is used for clarity). The bandstructure contains clearly-defined edge states whose dispersion curves have real parts nearly indistinguishable from the lossless network’s topological edge states. Apart from these, there also exist propagating bulk states. Even in the range of ϕ corresponding to the lossless network’s bulk bandgap, there are bulk states with $\text{Re}[k] \neq 0$, which are continuable to purely evanescent ($\text{Re}[k] = 0$) states of the lossless system. However, these bulk states have

significantly larger attenuation $|\text{Im}(k)|$ compared to the edge states, which can be attributed to the fact that they experience losses over a wider area. If we wind $\arg[r_{\pm}]$ through 2π , with fixed $|r_{\pm}| < 1$ (corresponding to a sub-unitary trajectory in the complex plane), the part of the complex projected bandstructure corresponding to the bulk states remains nearly unchanged, in both its real and imaginary parts. For the edge states, the real part of the dispersion curve winds with $\arg[r_{\pm}]$, whereas the imaginary part remains nearly unchanged. Hence, winding $\arg[r_{\pm}]$ has the effect of “pumping” a branch of lossy edge states across one quasi-energy period.

In summary, we have observed a topological invariant related to adiabatic pumping in a classical microwave network. Since networks of this sort are rather simple to set up, they can be used as a convenient platform for studying the physics of topological bandstructures. In particular, the quasi-energy bandstructures which arise in these networks are formally equivalent to the Floquet bandstructures that describe Floquet topological insulators [24–29]. In the square-lattice network of the present experiment, the topologically nontrivial phase is known to be an “anomalous Floquet insulator” phase, in which all bands have zero Chern number despite the presence of topological edge states [26]; in other network geometries, such as hexagonal lattice networks, various parameter choices would allow one to observe anomalous Floquet insulator, Chern insulator, as well as conventional insulator phases [20]. If couplers with tunable coupling strengths are implemented, the transitions between these various phases could be directly observed. In future work, it would be desirable to reduce the losses in the network components. Even at the current loss levels, however, the appearance of a non-zero winding number invariant is clearly observable. Based on our above arguments, the edge states are physically meaningful despite the presence of loss; although both edge states and bulk states undergo attenuation, the two types of state are clearly distinguishable in the complex projected bandstructure. The edge states receive significantly less attenuation, and are thus expected to be the dominant mode of transmission along the edge.

V. ACKNOWLEDGEMENTS

We are grateful to M. Hafezi, M. Rechtsman, C. Soci, and N. Zheudev for helpful discussions. This research was supported by the Singapore National Research Foundation under grant No. NRFF2012-02, and by the Singapore MOE Academic Research Fund Tier 3 grant MOE2011-T3-1-005.

-
- [1] M. Stone, *Quantum Hall Effect* (World Scientific, 1992).
 [2] J. E. Moore, Nature 464, 194 (2010).

- [3] F. D. M. Haldane and S. Raghu, Phys. Rev. Lett. **100**, 013904 (2008).

- [4] S. Raghu and F. D. M. Haldane, Phys. Rev. A **78**, 033834 (2008).
- [5] Z. Wang, Y. D. Chong, J. D. Joannopoulos, and M. Soljačić, Phys. Rev. Lett. **100**, 013905 (2008).
- [6] Z. Wang, Y. D. Chong, J. D. Joannopoulos, and M. Soljačić, Nature **461**, 772 (2009).
- [7] M. C. Rechtsman, J. M. Zeuner, Y. Plotnik, Y. Lumer, D. Podolsky, F. Dreisow, S. Nolte, M. Segev, and A. Szameit, Nature **496**, 196 (2013).
- [8] M. Hafezi, E. A. Demler, M. D. Lukin, and J. M. Taylor, Nature Phys. **7**, 907 (2011).
- [9] M. Hafezi, S. Mittal, J. Fan, A. Migdall, and J. M. Taylor, Nat. Photonics **7**, 1001 (2013).
- [10] K. Fang, Z. Yu, and S. Fan, Nature Phot. **6**, 782 (2012).
- [11] J. Koch, A. A. Houck, K. Le Hur, and S. M. Girvin, Phys. Rev. A **82**, 043811 (2010).
- [12] A. Petrescu, A. A. Houck, and K. Le Hur, Phys. Rev. A **86**, 053804 (2012).
- [13] A. B. Khanikaev, S. H. Mousavi, W.-K. Tse, M. Kargarian, A. H. MacDonald, and G. Shvets, Nature Materials **12**, 233 (2013).
- [14] K. v. Klitzing, G. Dorda, and M. Pepper, Phys. Rev. Lett. **45**, 494 (1980).
- [15] D. Thouless, M. Kohmoto, M. P. Nightingale, and M. den Nijs, Phys. Rev. Lett. **49**, 405 (1982).
- [16] R. B. Laughlin, Phys. Rev. B **23**, 5632 (1981).
- [17] P. W. Brouwer, Phys. Rev. B **58**, R10135 (1998).
- [18] D. Meidan, T. Micklitz, and P. W. Brouwer, Phys. Rev. B **84**, 195410 (2011).
- [19] I. C. Fulga, F. Hassler, and A. R. Akhmerov, Phys. Rev. B **85**, 165409 (2012).
- [20] M. Pasek and Y. D. Chong, Phys. Rev. B **89**, 075113 (2014).
- [21] Y. E. Kraus, Y. Lahini, Z. Ringel, M. Verbin, and O. Zilberberg, Phys. Rev. Lett. **109**, 106402 (2012).
- [22] M. Verbin, O. Zilberberg, Y. Lahini, Y. E. Kraus, and Y. Silberberg, arXiv:1403.7124.
- [23] M. Hafezi, Phys. Rev. Lett. **112**, 210405 (2014).
- [24] T. Oka and H. Aoki, Phys. Rev. B **79**, 081406 (2009).
- [25] J. Inoue and A. Tanaka, Phys. Rev. Lett. **105**, 017401 (2010).
- [26] T. Kitagawa, M. S. Rudner, E. Berg, and E. Demler, Phys. Rev. A **82**, 033429 (2010).
- [27] T. Kitagawa, E. Berg, M. Rudner, and E. Demler, Phys. Rev. B **82**, 235114 (2010).
- [28] N. H. Lindner, G. Refael and V. Galitski, Nature Physics **7**, 490-495 (2011).
- [29] Z. Gu, H. A. Fertig, D. P. Arovas, and A. Auerbach, Phys. Rev. Lett. **107**, 216601 (2011).
- [30] M. S. Rudner, N. H. Lindner, E. Berg, and M. Levin, Phys. Rev. X **3**, 031005 (2013).
- [31] J. T. Chalker, and P. D. Coddington, J. Phys. C **21**, 2665 (1988).
- [32] B. Kramer, T. Ohtsuki, and S. Kettemann, Phys. Rep. **417**, 211 (2005).
- [33] S. Ryu, C. Mudry, H. Obuse, and A. Furusaki, New J. Phys. **12**, 065005 (2010).
- [34] G. Q. Liang and Y. D. Chong, Phys. Rev. Lett. **110**, 203904 (2013).
- [35] G. Q. Liang and Y. D. Chong, Int. J. Mod. Phys. B **28**, 1441007 (2014).